coatings

MDPI

Article

Sintering Behavior, Microstructure and Microwave Dielectric Properties of Li_2TiO_3-Based Solid Solution Ceramics with Lithium Fluoride Addition for Low-Temperature Co-Fired Ceramic Applications

Yunfeng Guo, Zexing Wang and Jiamao Li *

Advanced Ceramics Research Center, School of Materials Science and Engineering, Anhui University of Technology, Ma'anshan 243032, China; guoyunfeng1101@163.com (Y.G.); w1512592461@163.com (Z.W.)
* Correspondence: lijiamao@ahut.edu.cn

Abstract: Nowadays, low-temperature co-fired ceramic (LTCC) technology has become one of the main forms of manufacturing electronic devices. However, a majority of microwave dielectric ceramics are not suitable as LTCC materials due to their high sintering temperatures. Developing novel LTCC materials with good microwave dielectric properties is extremely urgent. In this paper, an LiF sintering aid was added to $Li_2Ti_{0.8}(Co_{1/3}Nb_{2/3})_{0.2}O_3$ (LTCN) ceramics to explore new LTCC materials. The sintering behavior, microstructure and microwave dielectric properties of LTCN + x wt% LiF ceramics were investigated in detail. The results indicated that the addition of LiF increased the degree of disorder in the LTCN matrix, transforming it from a monoclinic to a cubic crystal system. The ceramics exhibited relatively dense and homogeneous microstructures at the sintering temperature of 950 °C as the LiF doping amount was not less than 2 wt%. By LiF doping, the quality factor ($Q \times f$) value was significantly enhanced due to the improved microstructure. Meanwhile, the temperature coefficient of resonant frequency (τ_f) of LTCN ceramics was successfully regulated to the near zero value owing to the negative τ_f characteristic of LiF. Excellent microwave dielectric properties of dielectric constant (ε_r) = 19.01, $Q \times f$ = 144,890 GHz, τ_f = −1.52 ppm/°C were obtained when the sample doped 3 wt% LiF was sintered at 950 °C for 3 h. Furthermore, the good chemical compatibility of the LTCN-3 wt% LiF ceramic with silver electrodes suggested that the ceramic was a potential material for LTCC applications.

Keywords: microwave dielectric properties; LTCC; Li_2TiO_3-based ceramics; sintering

Citation: Guo, Y.; Wang, Z.; Li, J. Sintering Behavior, Microstructure and Microwave Dielectric Properties of Li_2TiO_3-Based Solid Solution Ceramics with Lithium Fluoride Addition for Low-Temperature Co-Fired Ceramic Applications. *Coatings* **2023**, *13*, 1732. https://doi.org/10.3390/coatings13101732

Academic Editor: Roberto Teghil

Received: 7 September 2023
Revised: 28 September 2023
Accepted: 3 October 2023
Published: 4 October 2023

1. Introduction

In the material family, oxides have attracted much attention due to their excellent mechanical properties, physical properties, and chemical properties [1,2] and, therefore, have been widely used in the field of optoelectronics, catalysis and electronics. In recent decades, the rapid development of wireless communications has made microwave dielectric ceramic devices with oxide components, such as duplexers, dielectric filters and multiplexers, a new research hotspot [3–5]. Moreover, low-temperature co-fired ceramic (LTCC) technology, which occupies a crucial role in the integration and miniaturization of multilayer devices, has become one of the dominant forms of fabricating electronic devices, and has raised the requirements for microwave dielectric ceramics. In addition to excellent dielectric properties, LTCCs also require relatively low sintering temperatures (below the melting point of metal electrode) to ensure co-fire with metal electrodes such as silver (Ag) [6–9]. However, the majority of microwave dielectric ceramics have high sintering temperatures (>1000 °C) which are not suitable for LTCC applications. As a result, the development of new microwave ceramics with good dielectric properties and low sintering temperatures is extremely urgent.

Lithium (Li)-based rock salt materials have been widely investigated as candidate materials for microwave applications [5,10–12]. Among them, lithium metatitanate (Li_2TiO_3) is an excellent candidate due to its suitable dielectric constant and cheap raw materials [6]. However, its $Q \times f$ (Q = $\tan\delta^{-1}$, $\tan\delta$ and f refer to dielectric loss and resonant frequency, respectively) value (63,500 GHz) is relatively low due to Li volatilization caused by an excessively high sintering temperature and microstructure deterioration caused by an order–disorder phase transition [13]. To resolve this problem, the oxide doping method is generally used. For instance, Bian et al. [14] revealed that a small amount of magnesium oxide (MgO) doping could improve the $Q \times f$ value by lowering the ordering degree of Li_2TiO_3. Zhang et al. [15] revealed that the $Q \times f$ value of Li_2TiO_3 could be enhanced by increasing the packing fraction by doping small amounts of nickel oxide (NiO). However, doping single oxides to the ceramic matrix will not always work in the improvement of the τ_f value [16]. Recent studies have shown that complex ion doping can modulate the τ_f of Li_2TiO_3 but can improve the $Q \times f$ value. The replacement of Ti^{4+} ions with $(Mg_{1/3}Nb_{2/3})^{4+}$ ions not only inhibits the formation of cracks in the ceramic but also suppresses the reduction in Ti^{4+} ions and the diffusion of Li^+ ions, successfully increasing the $Q \times f$ value of Li_2TiO_3 from 63,500 GHz to 113,774 GHz, and adjusting the τ_f value from +20.3 ppm/°C to +13.38 ppm/°C [17]. Chen et al. and Zhang et al. have also made good progress in the study of $(Co_{1/3}Nb_{2/3})^{4+}$ and $(Al_{0.5}Nb_{0.5})^{4+}$ complex ions replacing Ti^{4+} ions, respectively [18,19]. Shortly afterwards, Zhan et al. developed novel microstrip antenna with remarkable wide temperature stability for millimeter wave applications by introducing 10.8 mol% LMTZN into the Li_2TiO_3 system [20]. However, the issue of the high sintering temperatures of Li_2TiO_3-based ceramics still does not have a suitable solution.

As we know, a common way of lowering the sintering temperature of Li_2TiO_3-based ceramics is adding glasses or oxides with a low melting point. For example, Chen et al. [20] used Li_2O-ZnO-B_2O_3 to decrease the sintering temperature of Li_2TiO_3 ceramics to 900 °C. Guo et al. [21] utilized boric acid (H_3BO_3) to lower the sintering temperature of $Li_2Ti_{0.8}(Cu_{1/3}Nb_{2/3})_{0.2}O_3$ from 1140 °C to 860 °C. $Li_2Ti_{0.75}(Mg_{1/3}Nb_{2/3})_{0.25}O_3$ ceramics with a near-zero τ_f value (+4.3 ppm/°C and −6.1 ppm/°C) and low sintering temperature (910 °C and 870 °C) have been successfully obtained after doping 2 wt% vanadium pentoxide (V_2O_5) and 1 wt% 0.6CuO–0.4B_2O_3 additions, respectively [22]. A sintering temperature below 950 °C (~790 °C) has been also obtained in a 1 wt% CuO–B_2O_3 doped $Li_2Ti_{0.98}Mg_{0.02}O_{2.96}F_{0.04}$–1 wt% niobium pentoxide (Nb_2O_5) ceramic system [23]. However, these low-temperature sintering aids, especially glass materials, would inevitably deteriorate the $Q \times f$ value of the matrix because of higher dielectric losses. In contrast, lithium fluoride (LiF), which has the same rock salt structure as Li_2TiO_3, exhibits a low sintering temperature (800 °C) and a high $Q \times f$ (78,800 GHz), making it well suited as a low-temperature sintering aid [24–27]. For example, Hao et al. [28] reduced the sintering temperature to 950 °C by adding 2.5 wt% LiF to Li_2TiO_3. Meanwhile, the $Q \times f$ of Li_2TiO_3 was improved because of the enhancement in the microstructure. The sintering temperatures of the fluorine oxides $Li_5Ti_2O_6F$ and $Li_7Ti_3O_9F$ were below 950 °C, and the $Q \times f$ values were also greatly improved [29,30]. In our previous work, the sintering temperature of $Li_2Ti_{0.9}(Zn_{1/3}Ta_{2/3})_{0.1}O_3$ was reduced to 950 °C using LiF as sintering aid, and a high $Q \times f$ value (110,090 GHz) was also obtained [31]. Therefore, it is a viable solution to use LiF as a low-temperature sintering aid for Li_2TiO_3-based ceramics.

On the one hand, it is obvious from Table 1 that the $Li_2Ti_{0.8}(Co_{1/3}Nb_{2/3})_{0.2}O_3$ ceramic has a higher $Q \times f$ compared with the others. On the other hand, the $Li_2Ti_{0.8}(Co_{1/3}Nb_{2/3})_{0.2}O_3$ with a positive τ_f value can be mixed with LiF to obtain a ceramic material with a near-zero τ_f value. Meanwhile, the sintering temperature of LTCN ceramics can be effectively decreased due to the low melting point (848 °C) of LiF. As far as we know, the effects of LiF additions on the sintering behavior, microstructure and microwave dielectric properties of $Li_2Ti_{0.8}(Co_{1/3}Nb_{2/3})_{0.2}O_3$ solid-solution ceramics have not been reported. For such a purpose, $Li_2Ti_{0.8}(Co_{1/3}Nb_{2/3})_{0.2}O_3$-$x$ wt% LiF (x = 1–5) ceramics were prepared by the solid-state reaction method in this paper. As expected, a novel microwave dielectric material with a low sintering temperature, high $Q \times f$ and near-zero τ_f was successfully obtained. Furthermore,

the sintering properties, microwave dielectric properties and chemical compatibility of the ceramics with silver electrodes were investigated in detail.

Table 1. Microwave dielectric properties of some Li_2TiO_3-based ceramics.

Ceramic System	ε_r	$Q \times f$ (GHz)	τ_f (ppm/°C)	Reference
$0.8Li_2TiO_3$-0.2MgO	19.2	106,226	+3.56	[14]
$0.8Li_2TiO_3$-0.2NiO	20.4	83,608	+1.97	[16]
$0.7Li_2TiO_3$-0.3ZnO	22.95	99,800	−32.7	[12]
$Li_2Ti_{0.8}(Cu_{1/3}Nb_{2/3})_{0.2}O_3$	18.3	77,840	+9.8	[21]
$Li_2Ti_{0.85}(Zn_{1/3}Ta_{2/3})_{0.15}O_3$	18.69	102,531	+11.8	[32]
$Li_2Ti_{0.85}(Mg_{1/3}Ta_{2/3})_{0.15}O_3$	19.48	80,005	+9.5	[33]
$Li_2Ti_{0.7}(Co_{1/3}Nb_{2/3})_{0.3}O_3$	21.3	110,000	0	[18]
$Li_2Ti_{0.7}(Al_{1/3}Nb_{2/3})_{0.3}O_3$	21.2	181,800	+12.8	[19]
$Li_2Ti_{0.7}(Mg_{1/3}Nb_{2/3})_{0.3}O_3$	19.01	113,774	+13.38	[17]
$Li_2Ti_{0.8}(Co_{1/3}Nb_{2/3})_{0.2}O_3$	18.83	102,500	+9.27	This work

2. Materials and Methods

2.1. Materials

Lithium carbonate (Li_2CO_3, 99.99%), titanium oxide (TiO_2, 99%), cobalt monoxide (CoO, 99%), niobium oxide (Nb_2O_5, 99.9%) and lithium fluoride (LiF, 99.99%) were provided by Aladdin Biochemical Technology Co., Ltd. (Aladdin Chemical Reagent Company, Shanghai, China).

2.2. Fabrication of LTCN + x wt% LiF Ceramics

Traditional solid-state reaction method was used to synthesize the LTCN + *x* wt% LiF ceramics. After drying in an oven, all raw materials were weighed stoichiometrically. The LTCN pre-sintered powder was obtained by wet milling in a nylon jar for 8 h using alcohol as solvent and yttria-stabilized tetragonal zirconia polycrystals (Y-TZP) balls as ball-milling medium. Subsequently, the slurry was dried at 80 °C for 4 h and calcined at 850 °C for 2 h to obtain the LTCN powder. The LTCN powder was crushed and 1–5 wt% LiF was added to it, respectively, and then ball milled again for 8 h. After drying the ball-milled powder, a 5 wt% concentration of polyvinyl alcohol (PVA) solution was added to increase its adhesion. The prefabricated powder was pressed into cylinders with a diameter and thickness of 10 mm and 5 mm, respectively. The cylinders were placed in an alumina crucible with a lid and covered with a powder of the same composition (to prevent evaporation of the volatile elements, lithium, cobalt and fluorine), heated to 600 °C for 2 h to expel PVA and sintered at 900–1000 °C for 3 h. Finally, to investigate the chemical compatibility of the LTCN + *x* wt% LiF ceramics, 20 wt% Ag powder was added to the ceramic powder, the mixture was pressed into sheets and then sintered at 950 °C for 3 h.

2.3. Structural and Properties Characterizations

The bulk density of the samples was determined by the Archimedes method (XS64, Mettler Toledo, USA) with a medium of deionized water. Analysis of the phase structure of the samples was carried out by X-ray diffractometry (Ultima IV, Rigaku Corporation, Showashima, Tokyo, Japan) operating at 30 mA and 45 kV with Cu Kα radiation in the range of 2θ angles from 15° to 75°. The microscopic morphology of the samples was observed by scanning electron microscopy (SEM, Mira3, Tescan, Czech) at an accelerating voltage of 30 kV and the elemental composition of the samples was analyzed by energy dispersive X-ray spectroscopy (EDS, AztecOne, Oxford Instruments, London, UK). The ε_r and $Q \times f$ values in microwave frequencies ranging from 8.0 to 12.0 GHz were measured by the Hakki–Coleman dielectric resonator method and cavity approach using vector network analyzer (N5230C, Agilent, Palo Alto, California, USA), respectively. The value of τ_f was calculated from the resonant frequencies f_{25} and f_{85} measured at 25 °C and 85 °C by Equation (1).

$$\tau_f = \frac{(f_{85} - f_{25})}{60 \times f_{25}} \times 10^6 \ (\text{ppm/°C}) \quad (1)$$

3. Results and Discussion

3.1. Phase Composition and Structure Analysis

The X-ray diffraction (XRD) patterns of LTCN + x wt% LiF (x = 0–5) ceramics sintered at 950 °C for 3 h are shown in Figure 1a. Meanwhile, the XRD pattern of the pure LTCN ceramic is presented in Figure 1 as comparison. It is obvious from Figure 1a that the transition from an ordered monoclinic phase to a disordered cubic phase occurs after LiF doping. That is, all LTCN + x wt% LiF ceramics present pure cubic Li_2TiO_3 phases (PDF # 03-1024). As shown in Figure 1b, the (200) peak shifts to a higher 2θ direction with increasing LiF content. This phenomenon should be attributed to the variation in lattice parameters according to the Bragg equation (Equation (2)):

$$n\lambda = 2dsin\theta \quad (2)$$

where d, θ, λ and n are the crystal spacing, Bragg angle, X-ray wavelength and number of reflection levels, respectively. The general formula for LTCN + x wt% LiF ceramics can be expressed as $Li_{(2-x)/(3-2x)}Ti_{(0.8-0.8x)/(3-2x)}Co_{(0.2/3-0.2x/3)(3-2x)}Nb_{(0.4/3-0.4x/3)(3-2x)}O_{(3-3x)/(3-2x)}F_{x/(3-2x)}$ based on the MgO-type rock salt structure. Therefore, the $[Li_{2/3}Ti_{0.8/3}(Co_{1/3}Nb_{2/3})_{0.2/3}]^{2+}$ ion with an effective ionic radius of 0.71 Å is replaced by the Li^+ ion with an effective ionic radius of 0.76 Å and the O^{2-} ion with an effective ionic radius of 1.4 Å is substituted by the F^- with an effective radius of 1.33 Å [34]. The substitution of cations increases the ionic radius by 0.05 Å and the replacement of anions decreases the ionic radius by 0.07 Å, which indicates a decrease in the net ionic radius of 0.02 Å. This type of substitution leads to a contraction of the lattice and a smaller spacing of the crystal planes, causing the diffraction peaks of the X-rays to be shifted to a higher angle. The calculated cell volumes of LTCN + x wt% LiF (x = 0–5) ceramics (see Table 2) also further confirm this phenomenon. Our result is consistent with the phenomenon in a LiF-doped Li_2TiO_3 system reported by Ding et al. [35].

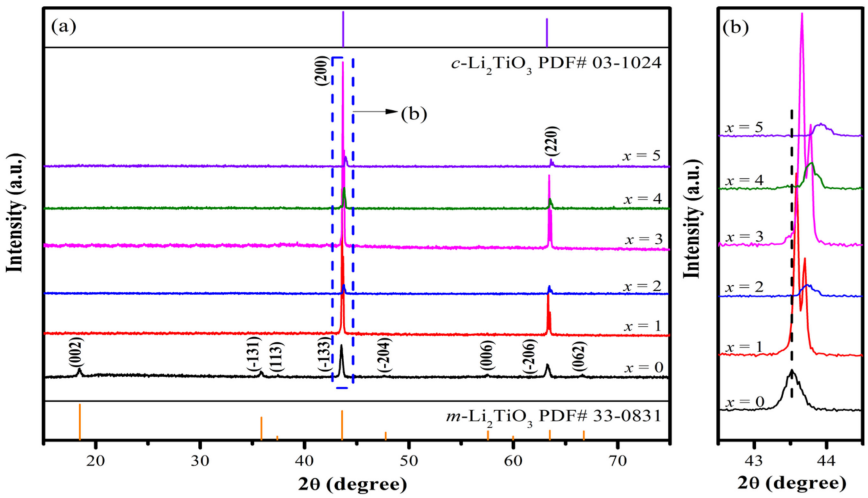

Figure 1. (**a**) XRD patterns of LTCN + x wt% LiF (x = 0–5) ceramics sintered at 950 °C, (**b**) amplified profile of the XRD patterns at 42.5°–44.5°.

Table 2. Lattice parameters and cell volumes of LTCN + x wt% LiF ceramics.

x Value	Lattice Parameter (a = b = c) (Å)	Cell Volume (Å^3)
1	4.1518(8)	71.570(9)
2	4.1516(7)	71.559(7)
3	4.1504(1)	71.495(0)
4	4.1495(4)	71.449(9)
5	4.1488(7)	71.415(1)

3.2. Density and Microscopic Morphology Analysis

Figure 2a shows the bulk density of LTCN + x wt% LiF ceramics (x = 1–5) sintered at different temperatures for 3 h. When adding 1 wt% LiF to LTCN ceramics, the density keeps increasing with the sintering temperature and still fails to densify at 1000 °C. When the doping amount rises to 2 wt%, the density rises significantly and the densification temperature of the ceramics is stable at 950 °C. This variation indicates that the doping of LiF has an outstanding effect on the sintering behavior of LTCN ceramics and successfully reduces the densification temperature of LTCN ceramics from 1300 °C to 950 °C. Figure 2b shows the diameter shrinkage of LTCN ceramic sintered samples at 950 °C for different LiF doping amounts. As the LiF doping amount increases from 1 wt% to 5 wt%, the diameter shrinkage shows an increasing and then decreasing trend, reaching a maximum value of 11% at x = 4. The apparent density shows a similar trend with the x value and reaches a saturation value of about 3.07 g/cm^3 at x = 4. The maximum density of the LTCN + 4 wt% LiF sample is higher than the density (< 2.97 g/cm^3) of Li_2TiO_3 that was synthesized from nano powders [36]. The increasing bulk density of LiF doping at 1–4 wt% can be attributed to the accelerated mass transport along the boundary by the formation of a liquid phase of LiF during the sintering process. When the LiF content is up to 5 wt%, the excess liquid phase can form too thick a film between the grains, which is counterproductive to mass transfer. That is, LiF mainly promotes the sintering performance of LTCN ceramics in two ways: On the one hand, it replaces O with F with a smaller effective ionic radius to weaken the oxygen bond strength and, hence, the intrinsic sintering temperature is reduced. On the other hand, it forms a liquid phase (with a melting point of 845 °C) during the sintering process to enhance the grain boundary mass transfer [28].

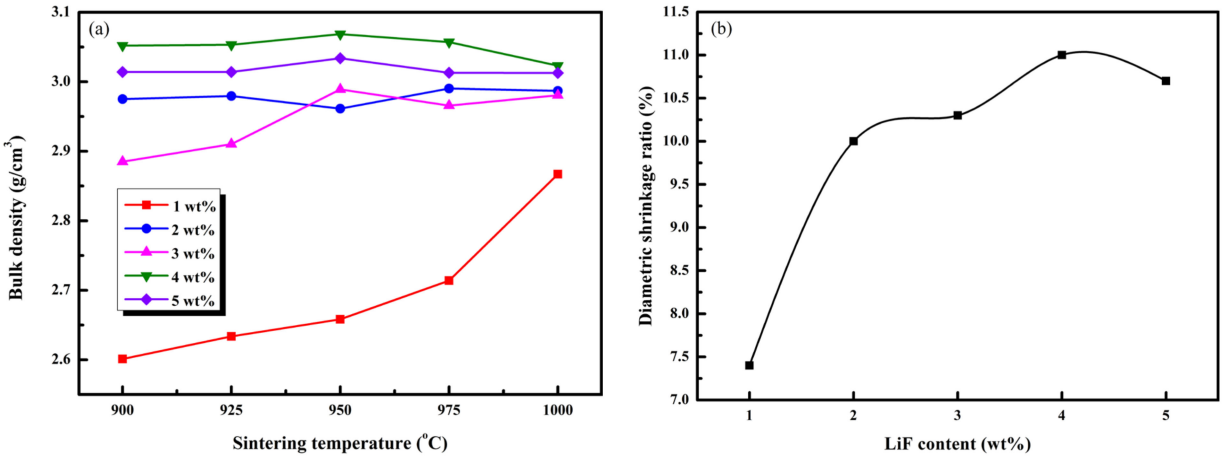

Figure 2. (**a**) bulk density of LTCN ceramics with different LiF contents sintered at 900–1000 °C for 3 h, (**b**) diameter shrinkage of LTCN + x wt% LiF ceramics sintered at 950 °C.

Figure 3 shows the SEM images and grain size distributions of LTCN ceramics sintered at 1300 °C for 3 h and LTCN ceramics doped with 1–5 wt% LiF sintered at 950 °C for 3 h, respectively. The grain sizes in the insets were obtained by measuring the grain size of at least 100 grains according to the linear intercept method using the Nano Measurer software. A significant increase in pores can be found after doping 1 wt% LiF into the LTCN ceramic, revealing that 1 wt% LiF is insufficient for densifying the ceramics at lower sintering temperatures, e.g., 950 °C. When the LiF doping amount is greater than 2 wt%, the microstructure of the samples becomes denser and clearer grain boundaries and a more uniform grain can be found. Figure 3a–f shows that a significant decrease in the average grain size [from 23.1 μm to (2.8–7.2) μm] occurs when the LiF is introduced due to the declined sintering temperature. In general, the higher the sintering temperature, the larger the average grain size for a given material composition. In addition, the average grain size increases with the increase in LiF content, increasing from 2.8 μm at x = 2 to 7.2 μm at

x = 5. This can be explained as large liquid phase accelerates the grain growth. A similar phenomenon has been reported in $Li_2MgTi_{0.7}(Mg_{1/3}Nb_{2/3})_{0.3}O_4$-doped LiF ceramics [37]. As a result, a moderate amount of LiF can significantly improve the microstructure of LTCN ceramics.

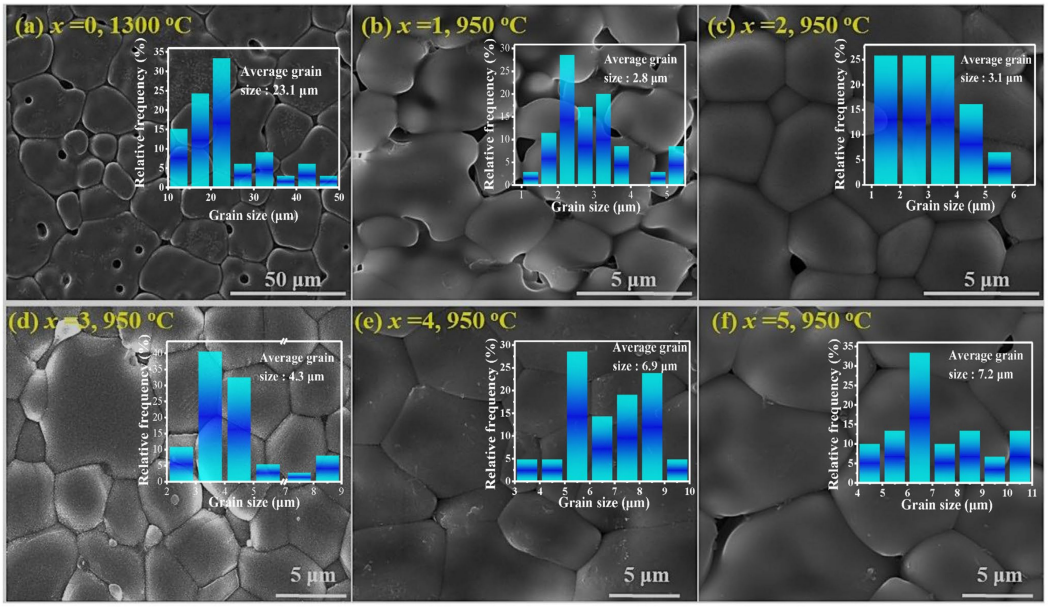

Figure 3. SEM images and average grain size distributions of LTCN + x wt% LiF (x = 0–5) ceramics: (**a**) x = 0, (**b**) x = 1, (**c**) x = 2, (**d**) x = 3, (**e**) x = 4, (**f**) x = 5.

The SEM images of 3 wt% LiF-doped ceramics sintered at 950 °C for 3 h and corresponding EDS element mapping results, except the Li element, are shown in Figure 4. It is evident that the oxygen (O), titanium (Ti), cobalt (Co), niobium (Nb) and fluorine (F) are uniformly distributed throughout the region and no segregation is observed in any region. The proportions of the elements in the inset of Figure 4g are close to the stoichiometric ratio.

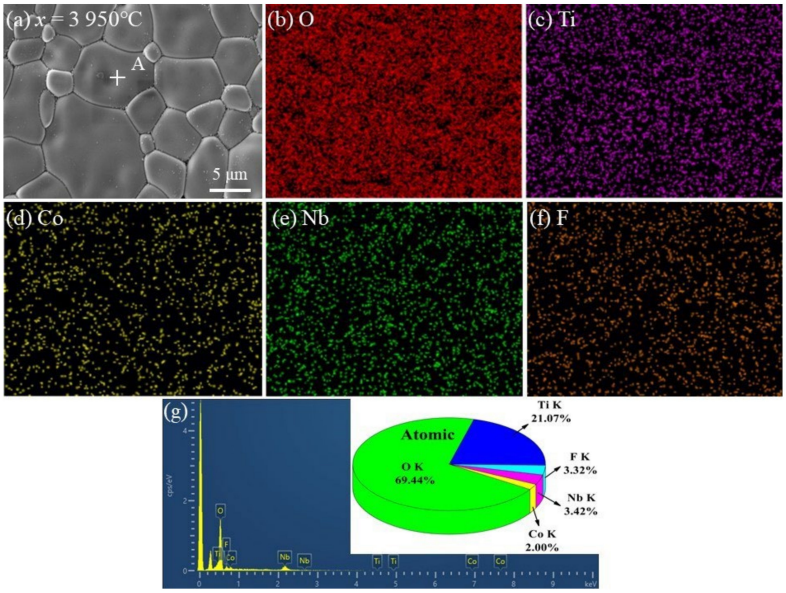

Figure 4. SEM images (**a**) of 3 wt% LiF-doped ceramic sintered at 950 °C for 3 h and corresponding EDS element mapping results of (**b**) O element (**c**) Ti element, (**d**) Co element, (**e**) Nb element, (**f**) F element and (**g**) EDS elemental analysis results of spot A.

3.3. Microwave Dielectric Properties Analysis

Figure 5a,b shows the ε_r and $Q \times f$ values of LTCN + x wt% LiF ceramics (x = 1–5) sintered at 900–1000 °C for 3 h, respectively. As can be seen, the trend of the dielectric constant as a function of the sintering temperature is consistent with the variation in the density in Figure 2, showing that the density is the main factor affecting the dielectric constant. A high density means that the number of pores with a low ε_r value ($\varepsilon_{r,air} \approx 1$) is reduced. However, the variation in the dielectric constant for different LiF doping amounts does not strictly follow the law of density variation. It is well known that in addition to density and phase composition, dielectric polarizability is a major influence on the dielectric constant of ceramics [38,39]. Here, the dielectric polarization rates of Li^+ (1.20 Å) and F^- (1.62 Å) are lower than $[Ti_{0.8}(Co_{1/3}Nb_{2/3})_{0.2}]^{4+}$ (2.98 Å) and O^{2-} (2.01 Å), respectively [40]. That is, the ε_r value should decrease gradually with the increasing LiF doping amount if the effect of density on the ε_r value can be ignored. Therefore, as shown by the dependence of ε_r on x in Figure 4a, it can be seen that the ε_r value of LTCN + x wt% LiF ceramics is determined by the density and dielectric polarizability.

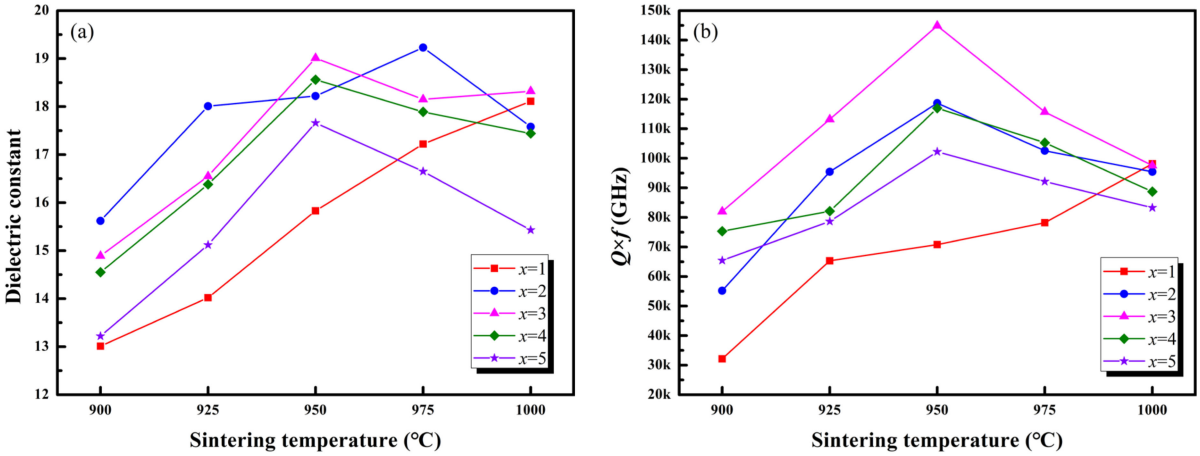

Figure 5. (**a**) ε_r values of LTCN + x wt% LiF ceramics sintered at 900–1000 °C for 3 h, (**b**) $Q \times f$ values of LTCN + x wt% LiF ceramics sintered at 900–1000 °C for 3 h.

It has been well documented that quality factors are closely related to density, grain size, second phase and crystal structure [41–43]. In this study, the trend of the $Q \times f$ value with sintering temperature is similar to that of the ε_r value. However, the $Q \times f$ value is not maximized at x = 4, which is the case of the density, but reaches a maximum value of 144,890 GHz at x = 3. This suggests that many factors other than density also have a significant effect on the $Q \times f$ value of LTCN + x wt% LiF ceramics. Since the second phase does not exist in LTCN + x wt% LiF ceramics, the effects of grain size and the amount of LiF doping are focused on. At $x \leq 3$, the increase in density and grain size plays a significant role in the improvement of the $Q \times f$ value. Previous studies have shown that the excessive addition of LiF has a significant negative effect on $Q \times f$ [31]. Therefore, the excess LiF causes a decreasing trend in the $Q \times f$ values of the ceramics as $x > 3$ [44]. However, the effect of all these factors on $Q \times f$ is difficult to quantify.

Figure 6 shows the variation in the τ_f value of LTCN + x wt% LiF ceramics sintered at 950 °C for 3 h. It is clearly seen that the τ_f value gradually decreases with the increase in LiF doping amount, mainly due to the moderating effect of LiF with a negative τ_f value (−135 ppm/°C) on LTCN with a positive τ_f value (+9.27 ppm/°C) [45,46]. In this study, the near-zero τ_f values are achieved at $2 \leq x \leq 4$, although the LiF doping amount has a significant effect on the $Q \times f$ values (Figure 5b). Therefore, the balance between the τ_f value and the $Q \times f$ value is important for practical applications of microwave dielectric ceramics. In summary, the LTCN + 3 wt% LiF ceramic sintered at 950 °C for 3 h exhibits good microwave dielectric properties of ε_r = 19.01, $Q \times f$ = 144,890 GHz and τ_f = −1.52 ppm/°C.

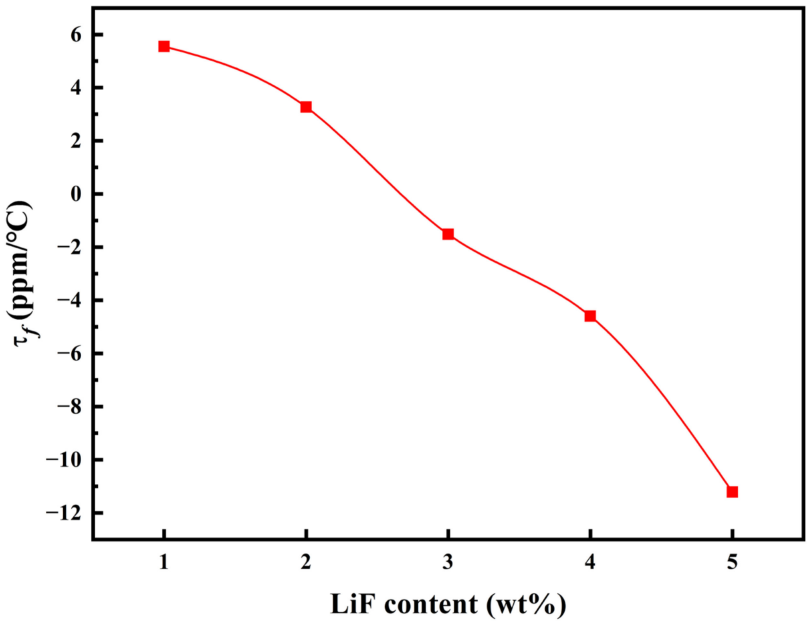

Figure 6. τ_f values of LTCN + x wt% LiF ceramics sintered at 950 °C for 3 h.

Table 3 provides a comparison of sintering temperatures and microwave dielectric properties of some ceramics with rock salt structures. Compared with other ceramics, the LTCN-3 wt% LiF ceramic has the best overall performance. Its $Q \times f$ value is significantly higher than that of the ceramics, except for the $Li_2MgTi_{0.7}(Mg_{1/3}Nb_{2/3})_{0.3}O_4$-3 wt% LiF ceramic, as shown in Table 3. However, the sintering temperature of the $Li_2MgTi_{0.7}(Mg_{1/3}Nb_{2/3})_{0.3}O_4$-3 wt% LiF ceramic is too high (1100 °C) to meet the requirements of LTCC technology. Therefore, the LTCN-3 wt%LiF ceramic is very competitive in rock salt structure compounds for LTCC applications because of its low sintering temperature and excellent microwave dielectric properties.

Table 3. Comparison of sintering temperature and microwave dielectric properties of some ceramics with rock salt structures.

Ceramic System	ST. (°C)	ε_r	$Q \times f$ (GHz)	τ_f (ppm/°C)	Reference
Li_2TiO_3-2.5 wt%LiF	950	24.01	75500	+36.2	[28]
$Li_2Ti_{0.9}(Zn_{1/3}Ta_{2/3})_{0.1}O_3$-3 wt%LiF	950	23.14	110,090	+3.25	[31]
$0.9Li_2TiO_3$-0.1LiF	1100	23.6	108,000	+4.2	[35]
$Li_2MgTi_{0.7}(Mg_{1/3}Nb_{2/3})_{0.3}O_4$-3 wt% LiF	1100	16.32	145,384	−16.33	[37]
Li_3TiO_3F	900	17.28	96,280	−32.7	[47]
$Li_5Ti_2O_6F$	880	19.6	79,500	−29.6	[29]
$Li_7Ti_3O_9F$	950	22.5	88,200	−24.2	[30]
$Li_4Mg_2NbO_6F$	900	15.53	93,300	−39.8	[48]
LTCN-3 wt%LiF	950	19.01	144,890	−1.52	This work

ST.: Sintering temperature.

3.4. Chemical Compliance with Silver Electrode Analysis

The chemical compatibility is an important criterion to determine whether ceramics can be used as LTCC materials. To study the chemical compatibility of LTCN + x wt% LiF ceramics, 20 wt% Ag powder was mixed with LTCN + 3 wt% LiF ceramic powder, these powders were pressed into the cylinder and were sintered at 950 °C for 3 h. The results of XRD, SEM and EDS elemental analyses of LTCN + 3 wt% LiF co-fired with silver are shown in Figure 7. It is obvious from Figure 7a that the XRD pattern matches well with the diffraction peaks of c-Li_2TiO_3 (PDF # 03-1024) and Ag (PDF # 04-0783), and no impurity

phase appears. From the inset of Figure 7a, the brighter A and the darker B are clearly separated. According to the EDS elemental analysis results of points A and B in Figure 6b, point A is the monolithic Ag and point B is the LTCN + 3 wt% LiF ceramic, implying that there is no chemical reaction between the ceramic and Ag. Hence, the LTCN + 3 wt% LiF ceramic is a promising material for LTCC applications.

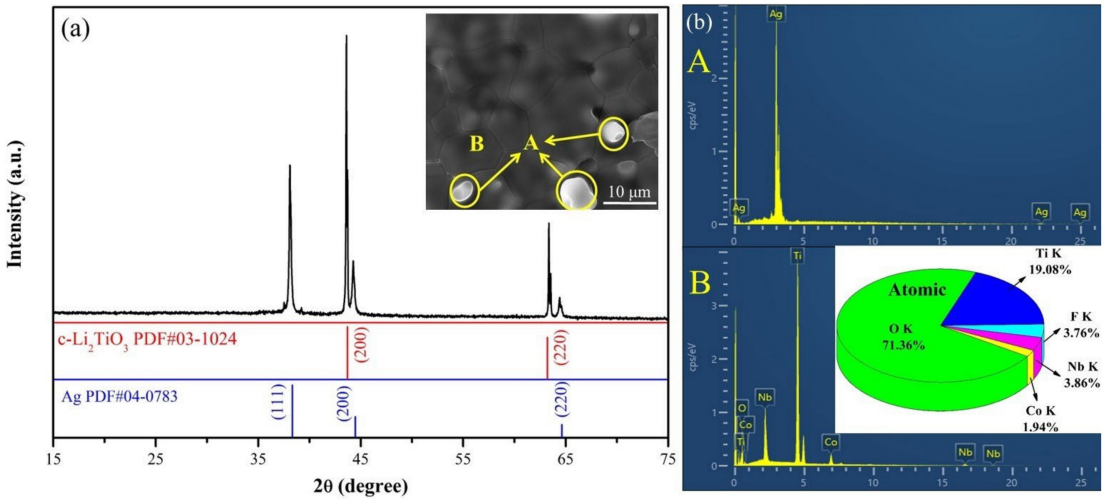

Figure 7. (**a**) XRD pattern and SEM image, (**b**) EDS elemental analysis results of points A and B in the co-fired ceramic.

4. Conclusions

In this paper, the phase structure, microstructure, microwave dielectric properties and chemical compatibility with Ag electrodes of LTCN + *x* wt% LiF ceramics were investigated. A continuous solid solution was formed throughout the entire range of LiF content. The addition of LiF transformed the LTCN matrix from an ordered monoclinic phase to a disordered cubic phase. By LiF doping, the sintering temperature of LTCN ceramics was effectively reduced to 950 °C and the quality factor ($Q \times f$) value was significantly enhanced due to the improved microstructure. Meanwhile, the τ_f of LTCN ceramics was successfully regulated to the near zero value, owing to the negative τ_f of LiF. Excellent microwave dielectric properties of ε_r = 19.01, $Q \times f$ = 144,890 GHz, τ_f = −1.52 ppm/°C were achieved for the LTCN + 3 wt % LiF ceramic sintered at 950 °C for 3 h. The chemical compatibility results showed that there is no chemical reaction between the ceramic and Ag. All results indicate that the LTCN + 3 wt % LiF ceramic is a promising material for LTCC applications.

Author Contributions: Conceptualization, J.L.; methodology, Z.W. and Y.G.; validation, J.L. and Z.W.; preparation, Y.G. and Z.W.; characterization, Y.G. and Z.W.; writing—original draft preparation, Y.G.; writing—review and editing, J.L.; supervision, J.L. All authors have read and agreed to the published version of the manuscript.

Funding: This work was supported by the Natural Science Foundation of Anhui Provincial Education Department (KJ2019A0054).

Institutional Review Board Statement: Not applicable.

Informed Consent Statement: Not applicable.

Data Availability Statement: All data are available from the corresponding author.

Conflicts of Interest: The authors declare no conflict of interest.

References

1. Masin, B.; Ashok, K.; Jayalatha, T.; Supriya, N.; Sreemoolanadhan, H.; Prabhakaran, K. A study of densification and enhanced microwave dielectric properties of Al_2O_3–polystyrene ceramic composites. *J. Electron. Mater.* **2023**, *52*, 6019–6030. [CrossRef]

2. Ahmad, T.; Ullah, B.; Lei, W.; Lu, W.Z. Band gap engineering and microwave dielectric properties evolution of mixed (Sr, La, Ce)$TiMgO_3$ titanate–aluminate system. *Ceram. Int.* **2023**, *49*, 6307–6313. [CrossRef]
3. Guo, W.J.; Ma, Z.Y.; Luo, Y.; Chen, Y.G. Structure, defects, and microwave dielectric properties of Al-doped and Al/Nd co-doped $Ba_4Nd_{9.33}Ti_{18}O_{54}$ ceramics. *J. Adv. Ceram.* **2022**, *11*, 629–640. [CrossRef]
4. Djouada, D.; Bouzit, N.; Delfouf, R.; Chioukh, L.; Martinez Jiménez, J.P. Dielectric characterization of heterogeneous composites using time domain spectroscopy and microwave test benches in microwave frequency. *ECS J. Solid State Sci. Technol.* **2023**, *12*, 063003. [CrossRef]
5. Bao, J.; Zhang, Y.P.; Kimura, H.; Wu, H.T.; Yue, Z.X. Crystal structure, chemical bond characteristics, infrared reflection spectrum, and microwave dielectric properties of $Nd_2(Zr_{1-x}Ti_x)_3(MoO_4)_9$ ceramics. *J. Adv. Ceram.* **2023**, *12*, 82–92. [CrossRef]
6. Ivetić, T.B.; Xia, Y.; Benzine, O.; Petrović, J.; Papan, J.; Lukić-Petrović, S.R.; Litvinchuk, A.P. Structure, electrochemical impedance and Raman spectroscopy of lithium-niobium- titanium-oxide ceramics for LTCC technology. *Ceram. Int.* **2021**, *47*, 4944–4953. [CrossRef]
7. Sarmento, J.S.; Paiva, D.V.M.; de Araújo, E.V.; Silva, M.A.S.; Sombra, A.S.B.; Mazzetto, S.E.; Fechine, P.B.A. Dielectric properties of $MCuSi_4O_{10}$(M = Ca, Sr, Ba) electro ceramic at RF and microwave frequencies. *Appl. Phys. A* **2023**, *129*, 72. [CrossRef]
8. Chen, G.H.; Xu, H.R.; Yuan, C.L. Microstructure and microwave dielectric properties of $Li_2Ti_{1-x}(Zn_{1/3}Nb_{2/3})_xO_3$ ceramics. *Ceram. Int.* **2013**, *39*, 4887–4892. [CrossRef]
9. Reda, A.E. Effect of ZnO on sintering and microwave dielectric properties of $0.5CaTiO_3$-$0.5(Li_{0.5}La_{0.5})TiO_3$ ceramics. *J. Indian Chem. Soc.* **2023**, *100*, 100901. [CrossRef]
10. Fu, Z.F.; Liu, P.; Ma, J.L.; Chen, X.M.; Zhang, H.W. New high *Q* low-fired $Li_2Mg_3TiO_6$ microwave dielectric ceramics with rock salt structure. *Mater. Lett.* **2016**, *164*, 436–439. [CrossRef]
11. Bi, J.X.; Li, C.C.; Zhang, Y.H.; Xing, C.F.; Yang, C.H.; Wu, H.T. Crystal structure, infrared spectra and microwave dielectric properties of ultra low-loss $Li_2Mg_4TiO_7$ ceramics. *Mater. Lett.* **2017**, *196*, 128–131. [CrossRef]
12. Huang, C.L.; Tseng, Y.W.; Chen, J.Y. High-Q dielectrics using ZnO-modified Li_2TiO_3 ceramics for microwave applications. *J. Eur. Ceram. Soc.* **2012**, *32*, 3287–3295. [CrossRef]
13. Bian, J.J.; Wang, L.; Yuan, L.L. Microwave dielectric properties of $Li_{2-x}Ti_{1-4x}Nb_{3x}O_3$ ($0 \leq x \leq 0.1$). *Mater. Sci. Eng. B* **2009**, *164*, 96–100. [CrossRef]
14. Bian, J.J.; Dong, Y.F. New high Q microwave dielectric ceramics with rock salt structures: $(1-x)Li_2TiO_3$ + *x*MgO system ($0 \leq x \leq 0.5$). *J. Eur. Ceram. Soc.* **2010**, *30*, 325–330. [CrossRef]
15. Zhang, J.; Zuo, R.Z. Low-temperature fired thermal-stable Li_2TiO_3–NiO microwave dielectric ceramics. *J. Mater. Sci. Mater. Electron.* **2016**, *27*, 7962–7968. [CrossRef]
16. Martins, V.C.; Oliveira, R.G.M.; Carmo, F.F.; Silva, M.A.S.; Pereira, S.A.; Goes, J.C.; Costa, M.M.; Gouveia, D.X.; Sombra, A.S.B. High thermal stability OF Li_2TiO_3-Al_2O_3 composite in the microwave C-Band. *J. Phys. Chem. Solids* **2019**, *125*, 51–56. [CrossRef]
17. Du, M.K.; Li, L.X.; Yu, S.H.; Sun, Z.; Qiao, J.L. High-*Q* microwave ceramics of Li_2TiO_3 co-doped with magnesium and niobium. *J. Am. Ceram. Soc.* **2018**, *101*, 4066–4075. [CrossRef]
18. Chen, W.S.; Hung, M.L.; Hsu, C.H. Effects of $(Co_{1/3}Nb_{2/3})^{4+}$ substitution on microstructure and microwave dielectric properties of $Li_2Ti_{1-x}(Co_{1/3}Nb_{2/3})_xO_3$ ceramics for applications in ceramic antenna. *J. Asian Ceram. Soc.* **2021**, *9*, 433–442. [CrossRef]
19. Zhang, T.W.; Zuo, R.Z.; Zhang, J. Structure, microwave dielectric properties, and low-temperature sintering of acceptor/donor co-doped $Li_2Ti_{1-x}(Al_{0.5}Nb_{0.5})_xO_3$ ceramics. *J. Am. Ceram. Soc.* **2016**, *99*, 825–832. [CrossRef]
20. Chen, G.H.; Yang, Y. Low-temperature sintering and microwave dielectric properties of Li_2TiO_3 based ceramics. *J. Mater. Sci. Mater. Electron.* **2013**, *24*, 1012–1017. [CrossRef]
21. Guo, H.H.; Fu, M.S.; Zhou, D.; Du, C.; Wang, P.J.; Pang, L.X.; Liu, W.F.; Sombra, A.S.B.; Su, J.Z. Design of a high-efficiency and -gain antenna using novel low-loss, temperature-stable $Li_2Ti_{1-x}(Cu_{1/3}Nb_{2/3})_xO_3$ microwave dielectric ceramics. *ACS Appl. Mater. Interfaces* **2021**, *13*, 912–923. [CrossRef] [PubMed]
22. Guo, H.H.; Zhou, D.; Du, C.; Wang, P.J.; Liu, W.F.; Pang, L.X.; Wang, Q.P.; Su, J.Z.; Singh, C.; Trukhanov, S. Temperature stable $Li_2Ti_{0.75}(Mg_{1/3}Nb_{2/3})_{0.25}O_3$-based microwave dielectric ceramics with low sintering temperature and ultra-low dielectric loss for dielectric resonator antenna applications. *J. Mater. Chem. C* **2020**, *8*, 4690–4700. [CrossRef]
23. Wang, D.; Li, L.X.; Du, M.K.; Zhan, Y. A low-sintering temperature microwave dielectric ceramic for 5G LTCC applications with ultralow loss. *Ceram. Int.* **2021**, *47*, 28675–28684. [CrossRef]
24. Song, X.Q.; Du, K.; Li, J.; Lan, X.K.; Lu, W.Z.; Wang, X.H.; Lei, W. Low-fired fluoride microwave dielectric ceramics with low dielectric loss. *Ceram. Int.* **2019**, *45*, 279–286. [CrossRef]
25. Tarakina, N.V.; Neder, R.B.; Denisova, T.A.; Maksinova, L.G.; Baklanova, Y.V.; Tyutyunnik, A.P.; Zubkov, V.G. Defect crystal structure of new $TiO(OH)_2$ hydroxide and related lithium salt Li_2TiO_3. *Dalton. Trans.* **2010**, *39*, 8168–8176. [CrossRef]
26. Fehr, T.; Schmidbauer, E. Electrical conductivity of Li_2TiO_3 ceramics. *Solid. State. Ion.* **2007**, *178*, 35–41. [CrossRef]
27. Bian, J.J.; Wu, J.Y.; Wang, L. Structural evolution, sintering behavior and microwave dielectric properties of $(1-x)Li_3NbO_4-xLiF$ ($0 \leq x \leq 0.9$). *J. Eur. Ceram. Soc.* **2012**, *32*, 1251–1259. [CrossRef]
28. Hao, Y.Z.; Yang, H.; Chen, G.H.; Zhang, Q.L. Microwave dielectric properties of Li_2TiO_3 ceramics doped with LiF for LTCC applications. *J. Alloys Compd.* **2013**, *552*, 173–179. [CrossRef]
29. Zhang, Z.W.; Tang, Y.; Xiang, H.C.; Yang, A.; Wang, Y.; Yin, C.Z.; Tian, Y.F.; Fang, L. $Li_5Ti_2O_6F$: A new low–loss oxyfluoride microwave dielectric ceramic for LTCC applications. *J. Mater. Sci.* **2020**, *55*, 107–115. [CrossRef]

30. Zhang, Z.W.; Fang, L.; Xiang, H.C.; Xu, M.Y.; Tang, Y.; Jantunen, H.L.; Li, C.C. Structural, infrared reflectivity spectra and microwave dielectric properties of the $Li_7Ti_3O_9F$ ceramic. *Ceram. Int.* **2019**, *45*, 10163–10169.
31. Liu, X.L.; Wang, Z.X.; She, X.Y.; Jia, Q.L.; Li, J.M. Improved microstructure and high quality factor of $Li_2Ti_{0.9}(Zn_{1/3}Ta_{2/3})_{0.1}O_3$ microwave ceramics with LiF additive for LTCC applications. *J. Eur. Ceram. Soc.* **2023**, *43*, 1469–1476. [CrossRef]
32. Liu, L.T.; Guo, W.J.; Yan, S.J.; Liu, P.; Du, J.L.; Zhang, Y.P.; Wu, H.T.; Chen, Y.G.; Yue, Z.X. Microstructure, Raman spectroscopy, THz time domain spectrum and microwave dielectric properties of $Li_2Ti_{1-x}(Zn_{1/3}Ta_{2/3})_xO_3$ ceramics. *Ceram. Int.* **2023**, *49*, 6864–6872.
33. Liu, L.T.; Guo, W.J.; Li, H.; Liu, P.; Qin, S.T.; Rong, X.X.; Liu, T.T.; Du, J.L.; Zhang, Y.P.; Chen, Y.G.; et al. The effect of $(Mg_{1/3}Ta_{2/3})^{4+}$ on the structure, Raman vibration, Terahertz time domain spectroscopy and dielectric properties for the Li_2TiO_3 ceramic. *Ceram. Int.* **2023**, *49*, 10186–10192. [CrossRef]
34. Shannon, R.D. Revised effective ionic radii and systematic studies of interatomic distances in halides and chalcogenides. *Acta. Cryst. A* **1976**, *32*, 751–767. [CrossRef]
35. Ding, Y.M.; Bian, J.J. Structural evolution, sintering behavior and microwave dielectric properties of $(1-x)Li_2TiO_3 + xLiF$ ceramics. *Mater. Res. Bull.* **2013**, *48*, 2776–2781. [CrossRef]
36. Jung, C.H. Sintering characterization of Li_2TiO_3 ceramic breeder powders prepared by the solution combustion synthesis process. *J. Nucl. Mater.* **2005**, *341*, 148–152. [CrossRef]
37. Yang, Y.K.; Liu, F.L.; Zhang, Y.W.; Li, M.F.; Liang, F.; Wu, H.T. Microwave dielectric properties of ultra-low loss $Li_2MgTi_{0.7}(Mg_{1/3}Nb_{2/3})_{0.3}O_4$ ceramics sintered at low temperature by LiF addition. *Ceram. Int.* **2018**, *44*, 12238–12244. [CrossRef]
38. Kumar, A.V.; Subramanian, V.; Sivasubramanian, V. Enhanced microwave dielectric properties of $ZnNb_2O_6$ by heterovalent ion substitution. *J. Alloys Compd.* **2023**, *944*, 169202. [CrossRef]
39. Kan, A.; Hirabayashi, R.; Takahashi, S.; Ogawa, H. Low-temperature crystallization and microwave dielectric properties of forsterite generated in $MgO–SiO_2$ system following LiF addition. *Ceram. Int.* **2023**, *49*, 9883–9892. [CrossRef]
40. Shannon, R.D. Dielectric polarizabilities of ions in oxides and fluorides. *J. Appl. Phys.* **1993**, *73*, 348–365. [CrossRef]
41. Wang, Z.X.; Guo, Y.F.; Li, J.M. Investigation on phase structure, spectral characteristics, microstructure and microwave dielectric properties of $Li_2Zn[Ti_{1-x}(Co_{1/3}Nb_{2/3})_x]_3O_8$ $(0.0 \leq x \leq 0.4)$ ceramics. *Ceram. Int.* **2023**, *49*, 15304–15314. [CrossRef]
42. Forghani, M.; Paydar, M.H.; Podonak, M.K.; Li, L. Microstructure and dielectric properties of novel $MgTiO_3$-*x*wt% $MgAl_2O_4$ microwave dielectric composite ceramics. *J. Mater. Sci. Mater. Electron.* **2023**, *34*, 690. [CrossRef]
43. Kumar, R.A.; Dutta, A.; Sinha, T.P. Structural and dielectric properties of microwave dielectric materials $xBa(Zn_{1/3}Ta_{2/3})O_3$-$(1-x)La(Zn_{1/2}Ti_{1/2})O_3$. *J. Electroceramics.* **2023**, *50*, 1–10. [CrossRef]
44. Liu, B.; Sha, K.; Jia, Y.Q.; Huang, Y.H.; Hu, C.C.; Li, L.; Wang, D.W.; Zhou, D.; Song, K.X. High quality factor cold sintered LiF ceramics for microstrip patch antenna applications. *J. Eur. Ceram. Soc.* **2021**, *41*, 4835–4840. [CrossRef]
45. Pulphol, P.; Vittayakorn, W.; Bongkarn, T.; Kolodiazhnyi, T.; Pongampai, S.; Maluangnont, T.; Vittayakorn, N. The tuning of temperature stability in ultralow loss (Ba/Sr) zirconate microwave dielectric. *Ferroelectrics* **2022**, *601*, 59–69. [CrossRef]
46. Gupta, R.; Kim, E.Y.; Shin, H.S.; Lee, G.Y.; Yeo, D.H. Structural, microstructural, and microwave dielectric properties of $(Al_{1-x}B_x)_2Mo_3O_{12}$ ceramics with low dielectric constant and low dielectric loss for LTCC applications. *Ceram. Int.* **2023**, *49*, 22690–22701. [CrossRef]
47. Wang, Z.X.; Guo, Y.F.; Li, J.M.; Li, C.H. A novel oxyfluoride ceramic in Li_2TiO_3–LiF system for LTCC applications. *Ceram. Int.* **2023**, *49*, 33425–33431. [CrossRef]
48. Zhai, S.M.; Liu, P.; Zhang, S.S. A novel high-Q oxyfluoride $Li_4Mg_2NbO_6F$ microwave dielectric ceramic with low sintering temperature. *J. Eur. Ceram. Soc.* **2021**, *41*, 4478–4483. [CrossRef]